

# Quasi Static Analysis of Microstrip Bondwire Interconnects

F. Alimenti (\*), U. Goebel (#), R. Sorrentino (\*)

(\*) Istituto di Elettronica, Università di Perugia, Italy, Phone: +39-75-5852658, Fax: +39-75-5852654.

(#) Deutsche Aerospace, Sedanstr. 10, 89077 Ulm, Germany, Phone: +49-731-3923415.

**Abstract**-A quasi-static approach for the analysis of microstrip bondwire interconnects is presented. The bondwire has been modelled as a cascade of inhomogeneous and nonuniform transmission lines, using the Conformal-Mapping method to determine the line characteristics and the theory of nonuniform transmission line to evaluate the effect of the variable height of the wire over the substrate.

## I. INTRODUCTION

A key element affecting the RF performances in microwave MIC modules is the microstrip bondwire interconnect. A typical assembly is shown in Fig.1; here two substrates, having different heights and permittivities, are placed on the same carrier with a certain air gap between the chips. Typically such interconnect is 300  $\mu\text{m}$  long, 200  $\mu\text{m}$  high and bonded with a 25  $\mu\text{m}$  diameter gold wire; the minimum achievable air gap is of the order of 100  $\mu\text{m}$ . Errors in placement of microstrip lines, mechanical tolerances of the carrier plates, and variations in wire bonding process, result in a not reproducible gap between substrates and produce wide variations in bondwire lengths.

In the past the microstrip bondwire was often modeled as a ribbon line [1] or even as a lumped element such as an inductor [2]. These models are suitable for short interconnection while become inadequate as the frequency increases since the wire exhibit transmission line properties. The analysis of a bondwire interconnect is a complicate 3D field problem because the structure is open and dielectric boundaries and bending of the wire are involved. A full-wave method requires a considerable numerical effort, thus of CPU time, to compute the performances of this discontinuity. In this paper a quasi-static approach for the analysis of microstrip bondwires is presented. The method consist of modelling the loop as a cascade of inhomogeneous and nonuniform transmission lines.

The work is organised in two parts. The first part presents the analysis of a uniform transmission line with a round wire over a ground plane coated with a dielectric

substrate. Line characteristics are obtained under the TEM approximation via the Conformal-Mapping method. The computed values of the effective dielectric constant have been checked against a Finite-Difference analysis.

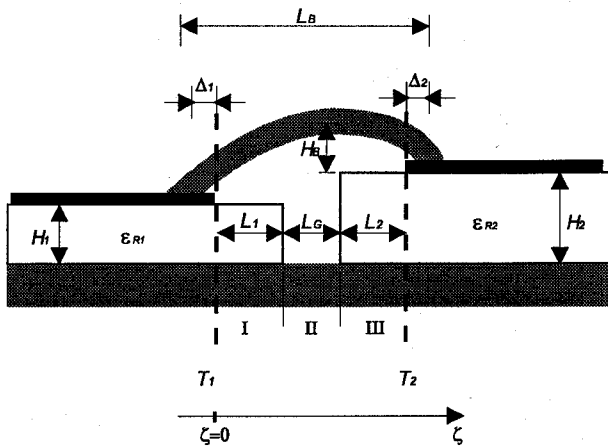


Fig.1. Bondwire interconnect. The loop inductance can seriously degrade performances of RF modules.

The effect of the variable height of the wire over the substrate is considered in the second part. The theory of nonuniform transmission lines is used leading to a complex Riccati's equation which is then solved numerically.

## II. CONFORMAL MAPPING ANALYSIS

The structure to be analysed consists of a circular wire over a ground plane covered with a dielectric layer. When symmetry is taken into account, the structure reduces to the geometry of Fig.2(a), where a magnetic wall is put on the symmetry plane  $y=0$ . The substrate has a thickness  $H$  and relative permittivity  $ε_r$ . The wire radius is  $R$  while the distance between its center and the ground is  $S$ . As shown in [3] the dispersion has a limited influence because of the small ratio between wire diameter and

WE  
3E

wavelength ( $2R/\lambda_0 < 0.01$  at 100 GHz). As a consequence a quasi-static approach is used to evaluate the characteristic impedance and effective permittivity of the line using the well known expressions:

$$\epsilon_{eff} = \frac{C}{C_0} \quad (1)$$

$$Z_c = \frac{1}{v_0 C_0 \sqrt{\epsilon_{eff}}} \quad (2)$$

where  $C$  and  $C_0$  are the line capacitances (per unit length) with and without dielectric substrate respectively, and  $v_0$  is the speed of light in a vacuum.

The Conformal-Mapping method has been used to compute these capacitances.

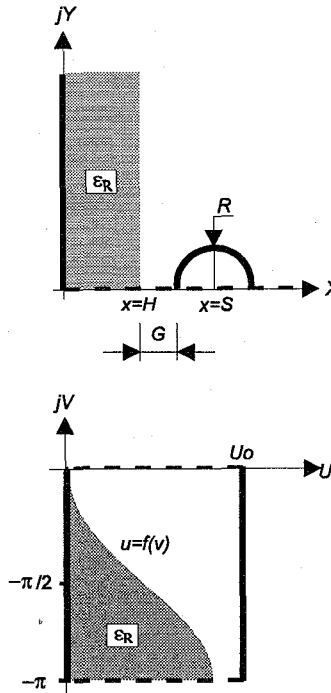


Fig.2(a), 2(b). A complex function maps half structure into a parallel plate capacitor partially filled of dielectric. Top and bottom magnetic walls are the images of the  $x$ -axis.

The substrate boundary, ground plane and round wire in the  $z$ -plane are transformed into a parallel plate capacitor with a curved dielectric inset in the  $w$ -plane, (Fig.2(a) and 2(b)), by the following complex function [4]:

$$w = \ln \left( \frac{z+a}{z-a} \right) \quad (3)$$

$$a = \sqrt{\left( \frac{S}{R} \right)^2 - 1} \quad (4)$$

The width of the capacitor in the  $w$ -plane is  $\pi$ , and the spacing between its metallization plates is  $U_0$ :

$$U_0 = \cosh^{-1} \left( \frac{S}{R} \right) \quad (5)$$

The capacitance of the air-filled line is simply given by:

$$C_0 = \epsilon_0 \frac{2\pi}{U_0} \quad (6)$$

A function  $u=f(v)$  represents the dielectric surface as the image, in the  $w$ -plane, of the straight line  $x=H$  of the  $z$ -plane.

The explicit form can be found by manipulating the equation (3):

$$f(v) = \tanh^{-1} \left( \frac{2P}{1 + P^2 + \frac{1}{\tan^2(v)} \cdot \left( \sqrt{1 + (1 - P^2) \cdot \tan^2(v)} + \delta \right)^2} \right) \quad (7)$$

where:

$$P = \frac{H}{\sqrt{\left( \frac{S}{R} \right)^2 - 1}} \quad (8)$$

and  $\delta$  indicates two different branches:

$$\delta = \begin{cases} +1, & v \in \left[ 0, -\frac{\pi}{2} \right] \\ -1, & v \in \left[ -\frac{\pi}{2}, -\pi \right] \end{cases} \quad (9)$$

The line capacitance  $C$  has been computed in the transformed plane by neglecting the field distortion due to the curved dielectric surface. Under this hypothesis the capacitor represented in Fig.2(b) can be sliced into infinitesimally thin pieces of width  $dv$  and its capacitance obtained as the sum of these elementary contributions. Such a procedure results in the following integral expression:

$$C = 2 \frac{\epsilon_0}{U_0} \int_{-\pi}^0 \left( 1 - \frac{1}{U_0} \left( 1 - \frac{1}{\epsilon_r} \right) \cdot f(v) \right)^{-1} dv \quad (10)$$

The assumption of no field distortion may appear to be rather strong. It is clearly reasonable whenever a low permittivity dielectric is used. However it has been found valid also for relatively high  $\epsilon_r$  ( $\approx 10$ ) as shown in section IV.

### III. NONUNIFORM TRANSMISSION LINE ANALYSIS

To complete our analysis of the bondwire, the latter is considered as the cascade of three nonuniform transmission lines (sections I, II, III of Fig.1). For any height of the wire over the substrate, the local characteristic impedance,  $Z(z)$ , and phase constant,  $\beta(z)$ , are computed at any point of the z-axis as shown in the previous section.

The input impedance  $Z_{in}$  of the bondwire is then obtained by solving the following complex Riccati's equation [5,6,7]:

$$\frac{dZ_{in}}{d\zeta} = -j \frac{\beta(\zeta)}{Z(\zeta)} Z_{in}^2 + j\beta(\zeta) Z_{in} \quad (11)$$

Note that in deriving the equivalent circuit, the reference planes (T1 and T2 of Fig.1) are located at the edges of the microstrip metallizations. Those portions of the microstrip that are located below the bond wire ( $\Delta_1$  and  $\Delta_2$  in Fig.1) have been neglected since their effect is expected to be very small.

To compute the impedance seen from T1 the structure has been closed on a reference impedance at T2, and then the equation (11) is integrated, numerically, with the fourth-order Runge Kutta algorithm. In the same way has been evaluated the impedance seen from T2. Since the bondwire has been considered lossless and reciprocal, the scattering parameters are computed directly from these impedances.

### IV RESULTS

To obtain the effective dielectric constant of the structure shown in Fig.2, the integral (10) has been computed using the Simpson's algorithm.

In order to verify the validity of the assumption that the dielectric inset produces a negligible field distortion, the line capacitance has also been evaluated using the 2D Finite-Difference method. The line cross-section was enclosed in a metallic box far enough from the wire, to avoid modifying the field distribution.

In Fig.3 and 4 the Conformal-Mapping and the Finite-Differences method are compared with reference [8]. These figures represent the effective dielectric constant ( $\epsilon_{eff}$ ) as a function of the normalised gap ( $G/R$ ), for  $\epsilon_r=9.6$  and for two values of the substrate thickness:  $H/R=10$  in

Fig.3 and  $H/R=20$  in Fig.4. Such ratios correspond to a 25  $\mu m$  diameter wire over a 125 or 254  $\mu m$  substrate.

The agreement between the Conformal-Mapping method and the Finite-Difference method is pretty good, while the model in [8] produces a large deviation when the wire is close to the substrate.

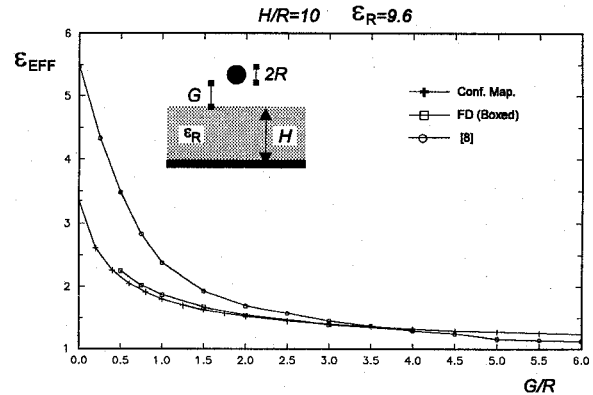


Fig.3. Effective dielectric constant versus the spacing between wire and substrate for  $H/R=10$  and  $\epsilon_r=9.6$ .

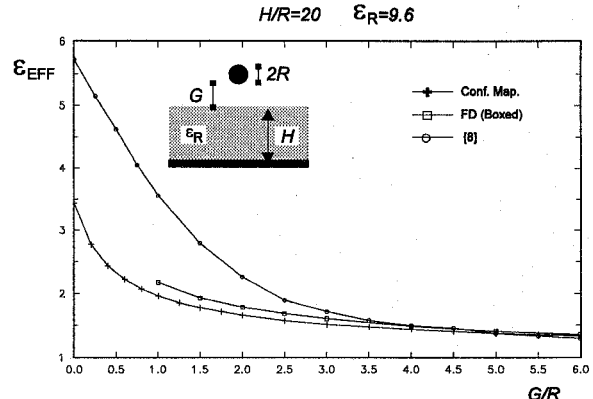


Fig.3. Effective dielectric constant versus the spacing between wire and substrate for  $H/R=20$  and  $\epsilon_r=9.6$ .

An example of bondwire interconnect analysis is presented now. The structure is a symmetric wire loop, bonding two  $50 \Omega$  microstrips. Only one chip with  $\epsilon_r=9.6$  is present. With reference to Fig.1 the mechanical dimensions are:  $H_1=H_2=100 \mu m$ ,  $L_G=0$ ,  $L_1=L_2=200 \mu m$ ,  $H_B=100 \mu m$  while the height of the wire over the substrate at the reference planes is 6  $\mu m$ . The wire diameter is 25  $\mu m$ .

Table-I represents the magnitude and phase of  $s_{11}$  and  $s_{21}$  at several frequency points. The matching of such interconnect is quite poor, hence it can seriously degrade the performances of RF modules and systems. The CPU time required for a complete analysis is of the order of one minute on a 486 PC.

Table-I

$f$ [GHz]	mag(s11)	arg(s11)	mag(s21)	arg(s21)
20	0.293	68.9	0.956	-20.1
40	0.516	52.7	0.857	-37.3
60	0.660	39.2	0.751	-50.8
80	0.748	28.7	0.664	-61.3
100	0.801	20.3	0.598	-69.7

Finally a simplified model of the bondwire has been derived. The local characteristic impedance and effective dielectric constant of the bondwire has been evaluated at the center and at one reference plane. An equivalent uniform line section has then been assumed having the average characteristic impedance and phase constant. The results are shown in Table II.

Table-II,  $Z_{av}=157\Omega$ ,  $\epsilon_{av}=1.63$ 

$f$ [GHz]	mag(s21)	arg(s21)
20	0.286	69.4
40	0.504	51.8
60	0.644	37.8
80	0.728	26.7
100	0.777	17.6

As can be seen, a good agreement is observed between the simplified uniform line model and the more rigorous nonuniform model; particularly with regard to the amplitude of the reflection coefficient.

## V. CONCLUSIONS

A quasi static analysis of microstrip bondwire interconnects has been developed using a Conformal-Mapping method to determine the transmission line characteristics and by solving, numerically, the Riccati's equation associated with the nonuniform configuration of the connecting wire. The CPU time required for a complete analysis is of the order of one minute on a 486 PC. The results on the line characteristics have been verified with a 2D Finite-Difference method and with published results. In the lack of reliable experimental data that will be performed soon, the computed scattering parameters of a bondwire interconnect have been compared with those obtained by an approximate model, showing a reasonable agreement.

## ACKNOWLEDGEMENTS

This work was done during a stage of F. Alimenti at Deutsche Aerospace (DASA) in Ulm, Germany, in the frame of the COMETT program. Dr. L. P. Schmitt and Dr. M. Bohem are acknowledged to their kind support.

## REFERENCES

- [1] H. Jin, R. Vahldieck, J. Huang and P. Russer, "Rigorous Analysis of Mixed Transmission line interconnects Using Frequency-Domain TLM Method," IEEE Trans. Microwave Theory Tech., vol. MTT-41, No.12, pp. 2248-2255, December 1993.
- [2] S. Nelson, M. Youngblood, J. Pavio, B. Larson and R. Kottman, "Optimum Microstrip Interconnections," IEEE MTT-S Int. Microwave Symposium Digest, pp. 1071-1074, June 1991.
- [3] N. Faché and D. De Zutter, "Full-Wave Analysis of a Perfectly Conducting Wire Transmission Line in a Double-Layered Conductor-Baked Medium," IEEE Trans. Microwave Theory Tech., vol. MTT-37, No.3, pp. 512-518, March 1989.
- [4] R. E. Collin, "Field Theory of Guided Waves," IEEE Press, pp.259-273 and page 324, New York, second edition, 1990.
- [5] M. J. Ahamed, "Impedance Transformation Equations for Exponential, Cosine-Squared and Parabolic Tapered Transmission Lines," IEEE Trans. Microwave Theory Tech., vol. MTT-29, No.1, pp. 67-68, January 1981.
- [6] P. Paramanic and P. Barthia, "Tapered Microstrip Transmission Lines," IEEE MTT-S Int. Microwave Symposium Digest, pp. 242-244, June 1983.
- [7] P. Paramanic and P. Barthia, "Analysis and Synthesis of Tapered Fin-Lines," IEEE MTT-S Int. Microwave Symposium Digest, pp. 336-338, June 1984.
- [8] R. H. Caverly, "Characteristic Impedance of Integrated Circuit Bond Wires," IEEE Trans. Microwave Theory Tech., vol. MTT-34, No.9, pp. 982-984, September 1986.
- [9] B. L. Lennartsson, "A Network Analogue Method for Computing the TEM Characteristics of Planar Transmission Lines," IEEE Trans. Microwave Theory Tech., vol. MTT-20, No.9, pp. 586-591, September 1972.
- [10] H. Shibata and R. Terakado, "Characteristics of Transmission Lines with a single Wire for a Multiwire Circuit Board," IEEE Trans. Microwave Theory Tech., vol. MTT-32, No.4, pp. 360-364, April 1984.
- [11] U. Goebel, "DC to 100 Ghz Chip-to-Chip Interconnects with reduced Tolerance Sensitivity by Adaptive Wirebonding," IEEE 3rd Topical Meeting on Electrical Performance of Electronic Packaging, Monterey, California, Nov. 2-4 1994, Proceedings pp. 182-185.